

Influence of moisture on the ferroelectric properties of sputtered hafnium oxide thin films

Fenja Berg,¹ Nils Kopperberg,¹ Jan Lübken,¹ Ilia Valov,² Xiaochao Wu,³ Ulrich Simon,³ and Ulrich Böttger¹

¹*Institute of Materials in Electrical Engineering and Information Technology 2, RWTH Aachen University*

²*Peter Gruenberg Institute 7, Research Centre Jülich*

³*Institute of Inorganic Chemistry and Electrochemistry, RWTH Aachen University*

(*Electronic mail: f.berg@iwe.rwth-aachen.de)

(Dated: 18 September 2023)

While the influence of various fabrication parameters during deposition on the ferroelectricity of hafnium oxide has been extensively studied, the effect of different atmospheres on the actual switching process has not yet been investigated. In this work, we characterized the ferroelectric properties of undoped hafnium oxide prepared by reactive sputtering under three different atmospheres: dry oxygen/nitrogen, wet nitrogen and vacuum conditions. We found a significant correlation between dry and wet atmospheres and the resulting polarization. Specifically, we observed a direct effect on the ferroelectric switching when the film was exposed to dry atmospheres and vacuum, resulting in a higher electric field necessary to initialize the wake up effect due to an initial imprint effect. Increasing the amount of wet nitrogen during the switching decreased the imprint and lowered the necessary voltage required for the wake up. We present a simple model that explains and discusses the incorporation of moisture and its resulting consequences on the ferroelectric properties of hafnium oxide. Additionally, Kinetic Monte Carlo simulations showed that the addition of protons to the oxide thin film leads to a lowering of the potential and to a redistribution of protons and oxygen vacancies which reduces the initial imprint.

I. INTRODUCTION

Integrated thin films of ferroelectric hafnium oxide, reported by Boeschke et al. in 2011¹, are promising candidates to overcome the drawbacks of conventional lead zirconate titanate (PZT) films, such as lack of CMOS compatibility and scalability^{2,3}. The ferroelectricity in hafnium oxide is attributed to a non-centrosymmetric orthorhombic phase which coexists with the known monoclinic, cubic and tetragonal phases^{4,5}. In 2018, a rhombohedral phase was reported in epitaxial thin hafnium zirconium oxide (HZO) thin films which also stabilizes the ferroelectric properties^{6,7}. For doped as well as undoped hafnium oxide, initial electrical cycling (wake up effect) plays an important role in stabilizing the ferroelectric phase by increasing the remanent polarization and opening a constricted hysteresis which is often observed in the pristine state^{8,9}. This effect is mostly explained by a field-driven redistribution of oxygen vacancies, which decreases an initially present built-in bias field and supports domain wall depinning within the layer. The defect redistribution is often observed to be accompanied by a field-driven phase transition to the ferroelectric orthorhombic phase^{10–14}. With further cycling the remanent polarization decreases again, known as the Fatigue effect, which has also been observed in conventional ferroelectrics like PZT^{15,16}. For undoped hafnium oxide, it has been reported that the influence of oxygen during deposition and annealing conditions is significant and directly affects the ferroelectric phase fraction and performance^{17–20}. However, the effect of different atmospheres, especially the effect of dry or humid atmospheres, during the wake up process has not been investigated yet. It has been shown in literature that moisture can significantly affect the electrical properties, especially in terms of resistive switching effects and conductivity for amorphous hafnium oxide films²¹.

In this paper, we report on detailed investigations and analysis of the influence of humidity on the ferroelectric characteristics of undoped hafnium oxide (HfO_x) for the first time. We conducted measurement series in vacuum, in mixed dry oxygen/nitrogen, dry pure nitrogen atmosphere and at different moisture partial pressures. While dry oxygen/nitrogen atmospheres, as well as vacuum, appear to prevent or delay the wake up effect at the same applied field, the addition of moist nitrogen during the switching process leads to the usual wake up effect and the formation of hysteresis, which has already been observed several times during measurements under ambient conditions.

We found a strong initial imprint effect due to internal fields that shifts the hysteresis along the voltage axis in one direction. With a positive voltage applied at to top electrode, the voltage shift is negative, shifting the coercive voltage in both positive and negative directions to lower voltages. Increasing the moisture content decreases the imprint and the internal field and results in the common observed wake up effect. In vacuum, a higher applied electrical field can compensate for the increased coercive voltage, leading to ferroelectric switching. In this work, a model for the influence of moisture on the internal bias field and coercive voltage is discussed. Kinetic Monte Carlo (KMC) simulations are applied to further investigate the effect of protons on the potential and thus the internal field responsible for the imprint.

II. EXPERIMENTAL DETAILS

The investigated film is prepared by reactive sputtering from an one inch metallic hafnium target at room temperature. The stack consists of a 30 nm platinum bottom electrode, a 25 nm thick HfO_x layer and a 50 nm platinum top electrode. The hafnium oxide is sputtered at an oxygen flow of 0.28 % and

a process pressure of 0.002 mbar at a constant power of 40 W. The platinum bottom electrode is prepared by sputtering at 150 °C, the top electrode at room temperature. The annealing procedure is performed in a rapid thermal annealing chamber (RTA) in nitrogen atmosphere at a temperature of 600 °C and with a 30 seconds holding time and a 10 seconds ramp. The process parameters have been examined before in Ref. 22.

The structural properties were investigated by Grazing Incidence X-ray Diffraction measurements (GI-XRD) with a Panalytical MPD Pro system. A Cu-K α wavelength from a copper x-ray tube is used to perform the measurements.

The electrical hysteresis characterization is performed with a Keithley 4200 at a frequency of 1000 Hz. The wake up pulses are implemented as square pulses, the hysteresis measurement is done by triangular pulses. For the wake up investigations, the pristine state of the cell was recorded before any wake up pulse was applied. The number of wake up cycles can be increased arbitrarily from 1 cycle to 10^7 cycles.

The humidity during the hysteresis and wake up measurements was measured with an analog humidity sensor. Diffuse Reflectance Infrared Fourier Transform Spectroscopy (DRIFTS) measurements were carried out with a VERTEX 70 FT-IR spectrometer from Bruker and Harrick Praying Mantis mirror system. Therefore, the HfO $_x$ sample were deposited on silicon dioxide (SiO $_2$) and the SiO $_2$ wafer was positioned on a ceramic sample holder with a resistive heating element at the back side for temperature control. The SiO $_2$ substrate was fixed by using conductive silver paste (PLANO GmbH) for heat conduction between the heating element and the substrate. A sketch of the ceramic sample holder and the measurement set up can be seen in Fig. S1 in the Supplementary Material. The ceramic substrate and the HfO $_x$ film were annealed for several hours at 120 °C in order to eliminate contributions from the silver paste in the following measurements. The temperature was chosen lower than the used crystallization temperature and the subsequent annealing temperature used in the electrical experiments to avoid affecting or changing the HfO $_x$ film and to provide the same experimental conditions. Afterwards, the ceramic substrate was placed inside a high-temperature reaction chamber (HVD-DRP, Harrick Scientific Products, Inc.) for in situ measurements. The temperature of the ceramic substrates was controlled via the back-side resistive circuit and a sourcemeter (Keithley). During the whole measurements, a dry nitrogen atmosphere with a flow rate of 20 mL/min $^{-1}$ was applied. The thin film was heated at 30 °C for 30 min, and the spectrum was recorded as background and subtracted from the spectra collected afterwards. Then the thin film was heated up to 390 °C gradually. The temperature steps amount to 20 °C and each temperature was hold for 15 minutes. The spectra were collected with the wavenumber range of 800-4000 cm $^{-1}$ simultaneously.

Leakage current measurements were performed with a Keithly 6430 and an additional current amplifier from Femto. The sweep rate was chosen to 0.8 V/min.

III. RESULTS AND DISCUSSION

For a structural characterization of the thin HfO $_x$ film GI-XRD measurements were carried out. HfO $_x$ thin films tend to crystallize in a combination of the tetragonal, the ferroelectric orthorhombic and the monoclinic phases. However, the similar peak positions of the tetragonal and orthorhombic phases make them indistinguishable using GI-XRD alone. Therefore, we only differentiate between the monoclinic and non-monoclinic phases. The crystal structure in FIG. 1 reveals a mixed phase consisting of a small monoclinic and a larger non-monoclinic phase fraction.

In Ref 22, a similar prepared HfO $_x$ thin film was characterized by further measurement method and an orthorhombic/tetragonal phase with some monoclinic phase content was found. The high non-monoclinic phase fraction in the GI-XRD measurement indicates good ferroelectric properties and a high remanent polarization.

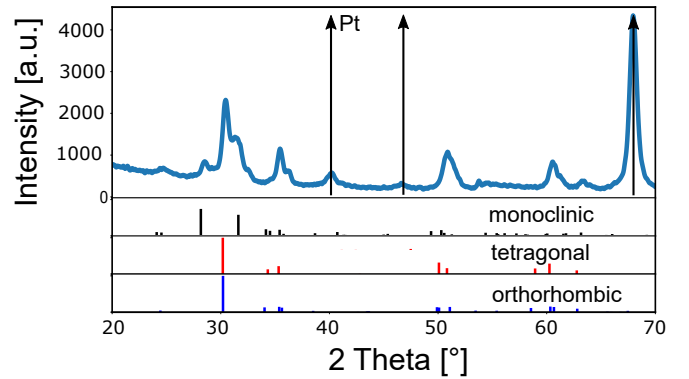


FIG. 1. GI-XRD measurement of the investigated thin HfO $_x$ film. The crystal structure is indicated by the diffraction pattern below. The contribution from the platinum electrode are marked by arrows.

A. Effects of different atmospheres

Further electrical measurements were performed to characterize the ferroelectric properties under different atmosphere conditions in a vacuum chamber which enables the control of the supply of moisture and the carrier gases: oxygen (O $_2$) and nitrogen (N $_2$). To create equal conditions, the different atmospheres were introduced according to the following scheme: (i) The normal investigated state in ambient atmosphere without evacuating the chamber, (ii) the evacuated state at $7 \cdot 10^{-6}$ mbar after 12 hours evacuation. In some cases, the sample had to be heated (170 °C for 1 hour) by an additional annealing element underneath the sample holder to achieve the chamber pressure. (iii) The dry state after evacuation, which was established by subsequent venting of the chamber by pure dry nitrogen or a mixture of 50 % dry nitrogen and 50 % dry oxygen or 30 % nitrogen and 70 % oxygen. The relative amount of residual humidity did not exceed 4 %. (iv) The wet state, which resulted from afterwards addition of wet nitrogen with different amounts of humidity between 27 % and 70 % into

the chamber. It should be noted that the vacuum chamber was evacuated every time before being filled with the different atmospheres or wet nitrogen. The corresponding current and hysteresis measurements for ambient atmosphere (i), vacuum (ii), and dry atmospheres (iii) are shown in FIG. 2 a) and b), respectively. For all measurements a wake up of 1000 cycles was performed.

The prepared ferroelectric hafnium oxide thin film has a $2P_r = P_{r+} - P_{r-}$ polarization value of about $18 \mu\text{C}/\text{cm}^2$ when the hysteresis measurement is performed in ambient air (scenario i)). In vacuum however, the characteristic ferroelectric switching peaks (see FIG. 2 a)) have almost completely disappeared and no hysteretic behavior is measured. When the vacuum is broken by adding dry nitrogen or a mix of dry nitrogen/oxygen, the measured relative humidity increases about time to a maximum humidity of 4 % due to the fact that the supplied gases are not completely dry coming out of the supply lines. With the slight increase in humidity, a small increase in polarization is recognizable, **which is enhanced compared to nitrogen when additional dry oxygen is added to the switching atmosphere**. However the polarization is still significantly reduced compared to measurements taken in ambient atmosphere.

Under vacuum, the remanent polarization seems to decrease the most, followed by dry nitrogen and a mixture of dry nitrogen and oxygen. However, the largest remanent polarization can be observed in ambient atmosphere leading to the conclusion that the moisture content of the environment seems to have a decisive influence on the ferroelectric properties. For detailed studies, investigations in humid atmospheres were carried out in a further experiment. For statistical reasons, several measurements were taken for each different humidity content and plotted in a boxplot in FIG. 3. The remanent polarization is extracted after a wake up of 1000 cycles. In the boxplot diagram, the median polarization is marked red, the box contains each 25 % larger and 25 % smaller measurement values than the median.

The addition of moisture during the switching process results in the formation of ferroelectric hysteresis with average remanent polarization values between $12 \mu\text{C}/\text{cm}^2$ (27 %), $16 \mu\text{C}/\text{cm}^2$ (50 %) and $20 \mu\text{C}/\text{cm}^2$ (70 %). There is a dependence of polarization on the moisture content of the atmosphere, since it increases significantly with increasing moisture content. The remanent polarization for switching in dry atmosphere amounts to comparatively lower values of $8 \mu\text{C}/\text{cm}^2$ and $11 \mu\text{C}/\text{cm}^2$.

B. Diffuse Reflectance Infrared Fourier Transform Spectroscopy measurement

From the measurements, we have concluded that moisture plays an important role during the actual ferroelectric switching process and promotes it. We performed DRIFTS measurements which provide information about the presence of water on the surface of the thin films. The DRIFTS spectrum is converted in Kubelka-Munk units to achieve a linear depen-

dency of the intensity on the amount of adsorbed species^{23,24}. The temperature programmed spectra in the range of $3000\text{--}4000 \text{ cm}^{-1}$ are shown in FIG. 4, which can be split into two parts: the temperature range from 30°C until 250°C (a) and from 270°C to 390°C (b). The characteristic broad bands at about 3250 cm^{-1} are observed, which can be assigned to the OH stretching modes^{25,26}. For the first temperature region, a small decrease in the bands intensity from 30°C until 250°C is recognizable indicating that OH species are detected from the surface and are most probably released by heating up the film until 250°C . In FIG. 4 b), the intensity starts to rise again for temperatures higher than 310°C up to 390°C . The cause of the renewed increase is not entirely clear. One possible explanation might be, that OH groups incorporated in the thin film have moved to the sample surface with increasing heating temperature. However, the exact origin of the second rise can not be completely clarified. In FIG. 4 c), the color map of the intensity in dependence of temperature (y-axis) and wavenumber (x-axis) is shown. As expected from the spectra shown before, between 200°C and 320°C no increased OH groups are detected which also indicates that the two OH contributions in the DRIFTS measurements could originate from two different processes taking place. Further confirmation, that water plays an important role could be seen in FIG. S3 in the Supplementary Material, which shows the hysteresis measurement of a sample heated in vacuum at 170°C for one hour compared to that of one without additional heating in vacuum. While the sample that was heated showed no apparent ferroelectric switching behavior, the sample measured in vacuum without additional heating exhibits a polarization of $5 \mu\text{C}/\text{cm}^2$. This decrease of remanent polarization with heating is a further strong indication that water plays an important role in our thin films during switching events.

C. Wake up effect

In FIG. 5, we show the temporal development of the switching current in vacuum, 27 % humidity, 50 % humidity and 70 % humidity for different numbers of wake up cycles along with the excitation voltage applied to the top electrode. FIG. 5 a) presents the switching current in vacuum for the pristine state, after 50 cycles, 600 cycles and 1500 cycles. No switching peaks can be detected after 50 and 600 cycles. At 1500 wake up cycles, a small increase in switching current is observed when a positive voltage is applied while no switching peak occurred for a negative applied voltage. In FIG. 5 b)-d) the measurements for 27 %, 50 % and 70 % humidity are shown. In contrast to vacuum, measurements in humid atmospheres show significant ferroelectric switching current peaks after 50 to 1500 wake up cycles.

Analyzing the change in the positions of the switching peaks with time, we find that in general, the negative coercive voltage in humid atmosphere shifts to smaller absolute voltage values with increasing cycling. For the positive coercive voltage, however, a shift to higher absolute voltages is observed. For a detailed investigation, in FIG. 6 the coercive voltage as well as the asymmetry of positive and negative

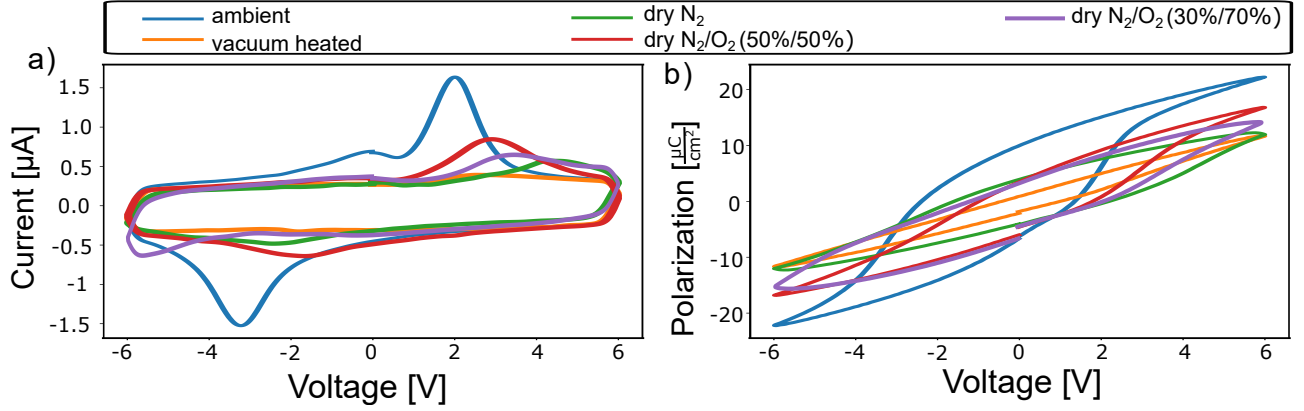


FIG. 2. a) Current measurements in ambient atmosphere, in heated vacuum and in dry oxygen and nitrogen atmosphere. b) Corresponding hysteresis.

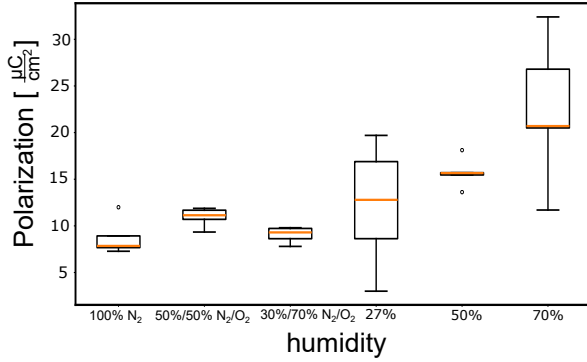


FIG. 3. Boxplot of polarization measured in different $p_{\text{H}_2\text{O}}$ partial pressures and in dry oxygen and dry nitrogen atmosphere with a relative humidity of 4%.

coercive voltage $\Delta V = V_{(c,+)} + V_{(c,-)}$ are extracted. At 27 % humidity and 50 wake up cycles, the negative coercive voltage is about -5 V while the positive coercive voltage is absolutely much lower at 1.9 V, resulting in a large difference ΔV . With increasing number of cycles, negative and positive coercive voltage values are approaching each other, resulting in a decrease in voltage shift from -2.7 V to -1.34 V at 1500 cycles. A similar trend can be seen for 50 % and 70 %. At higher humidity levels, however, the voltage asymmetry is less pronounced and voltage peaks are even visible in the pristine state, indicating that the film is already in a partly woken up state. Thus, increasing the amount of humidity results in a smaller voltage shift.

Based on the observation of the wake up effect we conclude that a strong asymmetry of the coercive voltage is present in the pristine state that is linked to an internal bias field. In case of the reverse of the external field, the coercive voltage shifts in the other direction (compare FIG. S2 in Supplementary Material), i.e. to higher absolute positive voltages and smaller absolute negative voltages, which confirms our assumption. Bias fields in thin hafnium oxide layers have been reported

before and can result from an asymmetric distribution of oxygen vacancies which accumulate at the electrode oxide interface. The resulting imprint behavior has been discussed and experimentally observed before in Ref. 27 and 28.

As the number of cycles during wake-up increases, the bias field is reduced, leading to an incipient wake-up effect and ferroelectric switching. In vacuum on the other hand, no distinct ferroelectric switching can be observed after 1500 cycles. The imprint effect is so pronounced that the applied voltage is not sufficient enough for a polarization reversal. An enhancement of the applied voltage repeals this restriction and leads to ferroelectric switching even under vacuum conditions (compare FIG. 6 b)). It should be taken into account that the higher applied electric field leads to a rise in the leakage current.

D. Model Explanation

In the following, we present a model explanation for the observed different behavior in wet and dry atmospheres. We suppose that the observed imprint effect due to the bias field present in the pristine state is caused by fabrication issues. In Ref. 29, it has been shown that annealing of HfO_x films with platinum top electrodes favors the formation of oxygen vacancies in oxygen-poor atmospheres. Consistently, we claim that for our samples annealed in pure nitrogen atmosphere oxygen vacancies accumulate at the interface between the hafnia film and the Pt top electrode forming an internal bias field across the oxide film (see FIG. 7 a)).

The decrease of the internal bias field and the imprint is attributed to a redistribution of defects in the thin film as it has been reported for oxygen vacancies during the wake up in Ref. 10. Since moisture enhances, accelerates or even enables the decrease of the **imprint**, we assume that not only oxygen vacancies play an important role for decreasing the imprint effect, but that hydroxide ions have a strong impact on the bias field, especially when lower fields are applied. Therefore, the electrochemical processes that could occur during switching in presence of H₂O molecules are discussed below. In Ref.

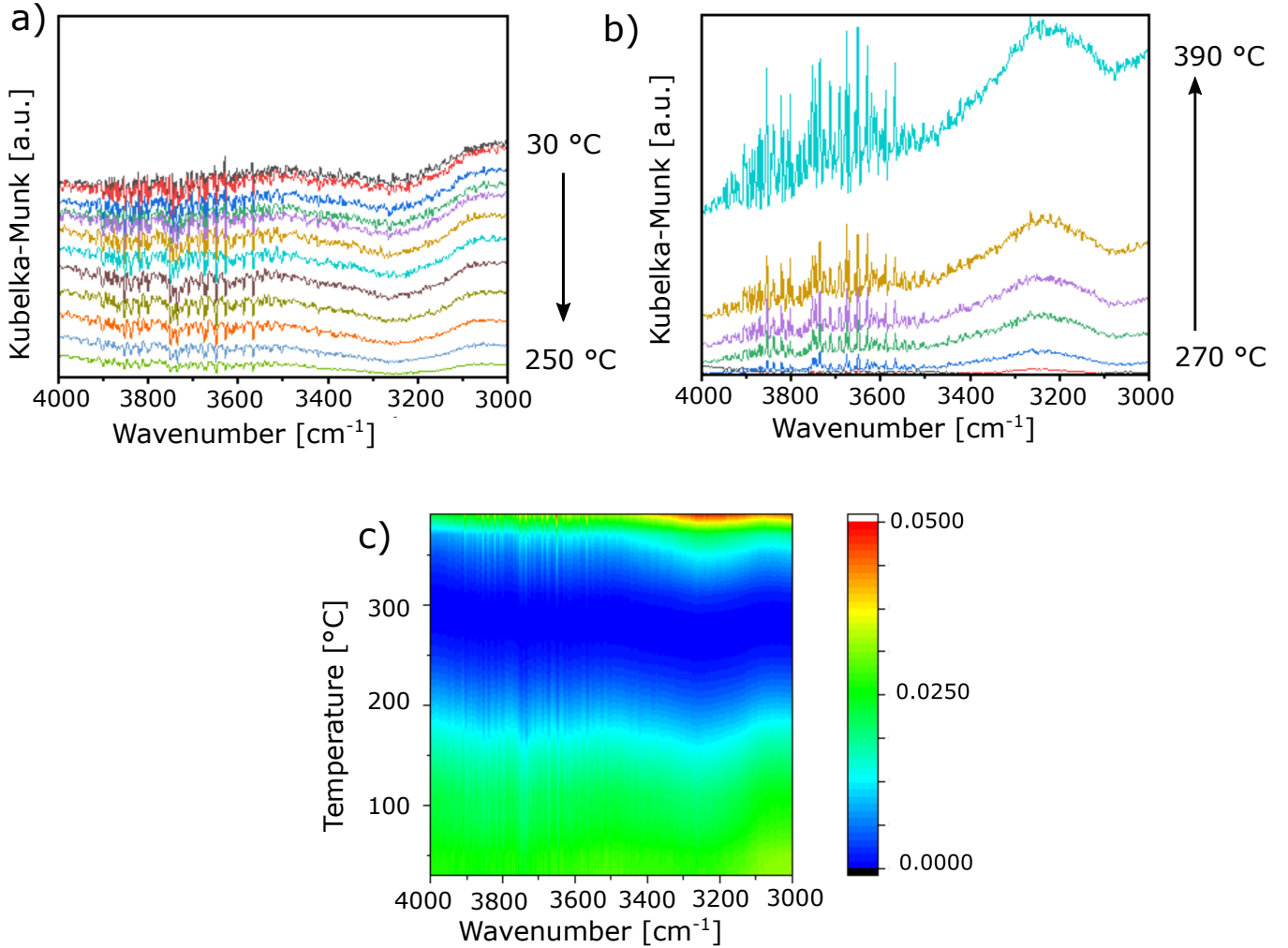
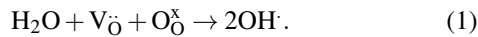


FIG. 4. In-situ temperature programmed DRIFTS measurements of thin HfO_x . The O-H band is located between 3000 and 3300 cm^{-1} . DRIFTS results for a) temperatures from 30 °C to 250 °C, b) temperatures from 270 °C to 350 °C. c) Color map of the measured intensity in dependence of temperature and wavenumber.

21, 30, and 31 it has been shown that moisture has a crucial impact on crystalline and amorphous oxide layers. In dense crystalline materials the incorporation of moisture can occur at the grain boundaries **due to the chemical potential gradient** by the dissolution of water into OH^- and H^+ via the following equation using the Kroeger-Vink notation



According to reaction (1), $\text{V}_{\text{O}}^{\bullet\bullet}$ refers to a double positively charged oxygen vacancy in relation to the lattice, $\text{O}_{\text{O}}^{\times}$ is the neutral oxygen ion on its regular lattice position and OH^{\cdot} represents a single positively charged proton sited on an oxygen ion. In the presence of moisture, one oxygen vacancy is occupied by an OH^- ion and a proton is bond to an oxygen atom on an oxygen site resulting in two single positively charged OH^{\cdot} ions relative to the lattice.

We assume that the OH^- accumulate at the top interface when

exposed to humid air. This suggestion is supported by the surface sensitive DRIFTS measurements which show an increase in intensity for the first temperature range when OH may be released from the interface. When an external electric field is applied, the protons bond to an oxygen atom may begin to redistribute.

In literature, few information about the mobility of hydrogen species in HfO_x are available. However, for yttrium stabilized zirconium oxide (YSZ) different studies of proton mobility have been reported. In Ref. 32 it was found that the grain boundaries of nanocrystalline YSZ are conductive for proton transport at room temperature. With increasing temperature, the conduction is reduced due to desiccation. The calculation of activation energies for proton mobility at the grain boundaries of crystalline YSZ exhibits values between 0.03 eV and 1.7 eV, depending on the chosen path of the proton³³. Under the influence of an electric field we suppose that protons

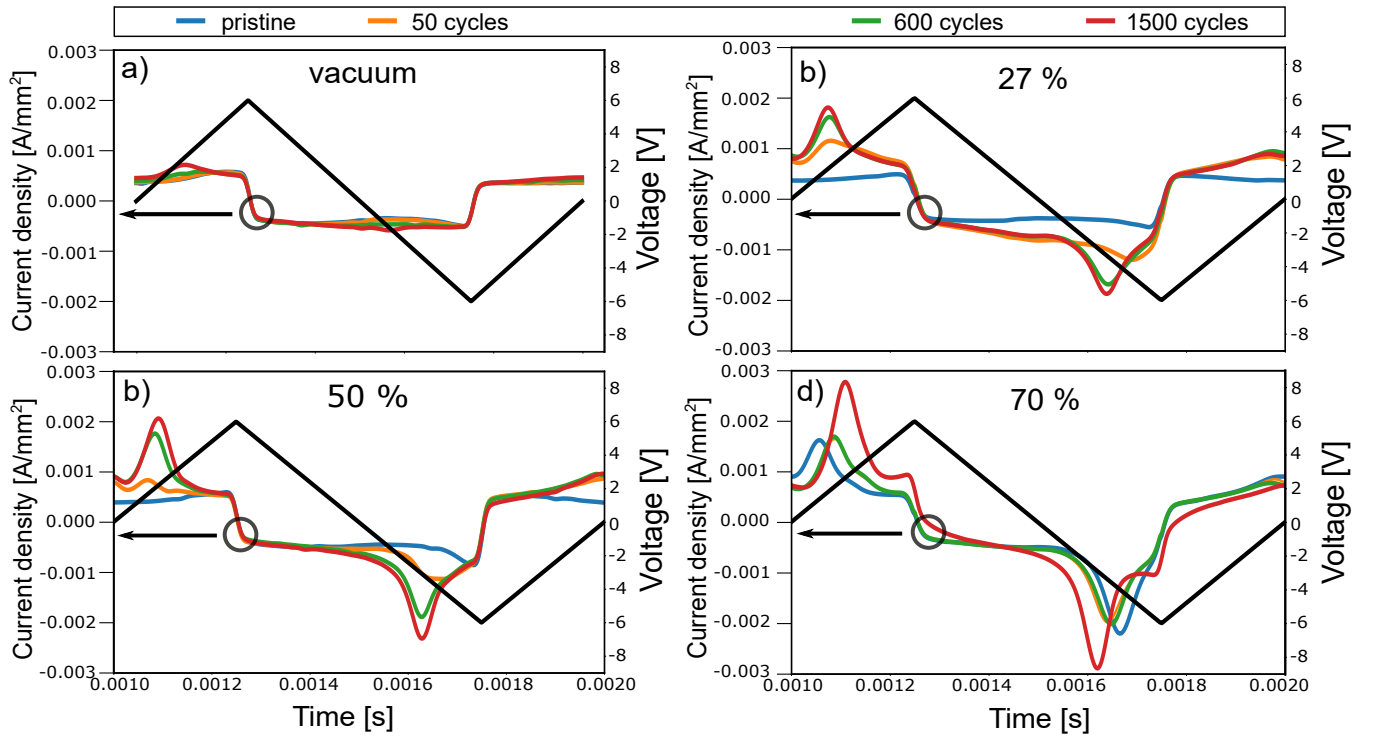


FIG. 5. Time development of the switching current in dependence of electrical cycling. Measurements taken in a) vacuum, b) 27 % humidity, c) 50 % humidity and d) 70 % humidity.

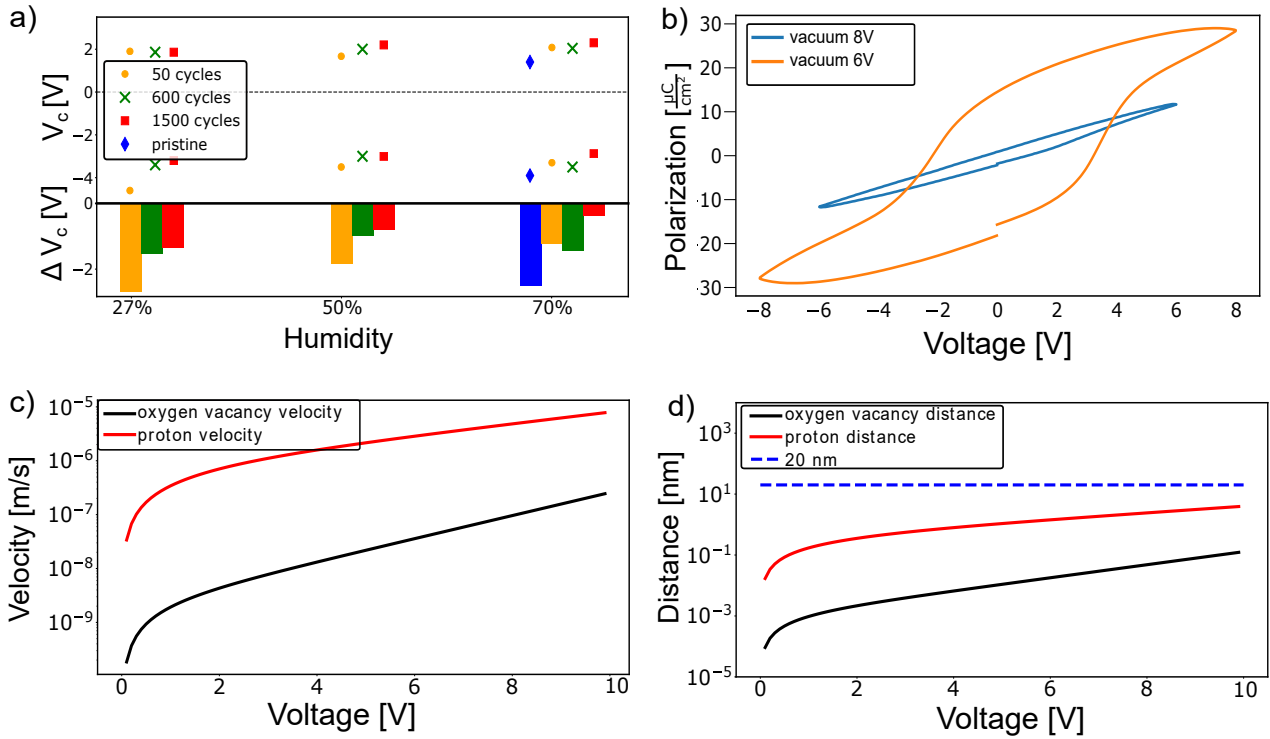


FIG. 6. a) Development of coercive voltage for different wake up cycles and different amounts of humidity (upper part). Asymmetry of the switching peaks as voltage shift (lower part). b) Hysteresis measured in vacuum for 6 V and 8 V excitation voltage. c) Oxygen vacancy and proton velocity calculated by Mott-Gurney equation. d) The distance covered by protons and oxygen vacancies as a function of the applied voltage calculated for a time of 0.5 ms.

hop from one oxygen ion to another and migrate through the crystal, which leads to a more uniform distribution of the positively charged protons and to a decrease of the internal bias field. Since a higher field is necessary for the redistribution of charges without moisture present, we conclude that protons are more mobile than oxygen vacancies, which leads to a faster decay of the internal field.

In Ref. 13 the velocity of oxygen vacancies during the wake up effect has been approximated by the Mott-Gurney equation³⁴

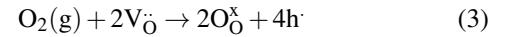
$$v = 0.5 \cdot af \exp\left(-\frac{W_0}{k_B T}\right) \sinh\left(\frac{za}{2k_B T} E\right) \quad (2)$$

where W_0 is the activation energy, a is the hopping distance, f the attempt frequency, z the ion's charge and E the electric field. Using values measured by Zafar et al.³⁵ ($a=0.25$ nm, $f=1 \cdot 10^{14} \text{s}^{-1}$, $z=2$) and an activation energy of 0.75 eV for oxygen vacancies (activation energies between 0.7 eV and 0.85 eV have been reported^{36,37}), as well as an activation energy of 0.6 eV and $z=1$ for protons (activation energies have been measured between 0.5 eV and 0.6 eV for YSZ^{38,39}) the velocities at room temperature $T=295$ K are illustrated in FIG. 6 c) as a function of the applied voltage. Considering that the AC-voltage is applied for 0.5 ms for each polarity using a frequency of 1 kHz, the migration distance can be calculated in dependence of the electric field and the results are shown in FIG. 6 d). A strong dependence of the velocity on the applied voltage is evident. When the internal bias field is aligned in the same direction as the external field, the effective field $E_{int} + E_{ext}$ driving the ions is larger than in the opposite direction. Therefore, the velocity of protons and oxygen vacancies is enhanced in direction of the bias field resulting in a net drift from the top electrode to the bottom electrode. Due to the smaller activation energy, the velocity is larger for protons compared to oxygen vacancies. After the protons have been incorporated at the interface in the hafnium oxide layer (see FIG. 7 b)), the protons start to redistribute uniformly within the oxide layer under the AC field leading to a reduction of the internal field and a lowering of the coercive voltage for the opposite direction (see FIG. 7 c)). This is also reflected in the electrical hysteresis measurements (cf. Fig. 6 a)), where only the application of an external field leads to a lowering of the bias field over time and subsequently to the uniformly migration of protons within the oxide. Moreover, Fig. 6 a) also strongly suggests that an increase in humidity level leads to an accelerated incorporation or to more incorporated protons resulting in a faster decay of the internal bias field.

At this point we would like to point out that the model introduced in this work is based on the case that the fabrication-related internal bias field is directed from the top electrode to the bottom electrode. We assume that due to the annealing process in nitrogen, oxygen vacancies accumulate at the top electrode which results in the ascribed bias field. However, if a different oxygen vacancy distribution is present in the thin film, e.g. an accumulation at the bottom electrode interface, this could lead to a different oriented bias field. In this precise case, the field would be directed from the bottom electrode to the top electrode. The resulting effective field

($E = E_{bias} + E_{ext}$) is enhanced in direction from the bottom to the top electrode which would not favor a redistribution of protons from the top interface into the layer. Consequently, we assume that for this case higher fields, as in vacuum, would be required to redistribute the oxygen vacancies and observe ferroelectric switching. However, since we did not observe an internal bias field directed from bottom to top interface in any of our prepared samples, no experimental results could be obtained for this case.

Influence of oxygen on the bias field



where $\text{O}_2(\text{g})$ is oxygen in the gas phase, $\text{V}_{\text{O}}^{\bullet\bullet}$ a doubly positively charged oxygen vacancy, $\text{O}_{\text{O}}^{\times}$ a neutral oxygen atom on its regular lattice position and h^{\bullet} a positively charged hole with respect to the lattice.

Subsequently, the incorporation of oxygen could lead to a decrease of the oxygen vacancy concentration at the interface and similarly to moisture to a reduction of the internal bias field and to lower voltages necessary to switch the ferroelectric film. Therefore, the incorporation of oxygen into the hafnium oxide film is discussed below.

First, it must also be considered that the oxygen and nitrogen from the supply lines will increase the humidity in the chamber to a maximum of 4 % over time. This increase in humidity can already lead to changes in the coercive voltage and polarization. Therefore, the effects of oxygen and humidity cannot be considered to be completely independent. On the other hand, however, there is a clear difference between dry nitrogen and oxygen, indicating that dry oxygen also has an effect on the internal field due to oxygen incorporation, although the resulting ferroelectric polarization is much lower than in case of moisture. In Fig. S5 in the Supplementary Material, the switching current in dry oxygen atmosphere for different number of wake up cycles is shown, similar to the measurements taken in moisture (compare Fig. 5). In contrast to wet atmospheres, except for the pristine state, only very slight differences in the coercive field and in the switching peaks can be identified for the different wake up states. This behavior indicates that as electrical cycling continues, additional oxygen is no longer incorporated.

In literature, reports about the incorporation of OH and H as well as the incorporation of oxygen can be found^{21,40–42}. However, the incorporation of oxygen into hafnium oxide has been described only for temperatures above room temperature, which are experimental conditions that were not met in our work. In addition, especially in⁴³, the authors point out that the effect of oxygen incorporation is significantly reduced for 22 nm HfO_x which has been annealed and crystallized before in nitrogen atmosphere. In contrast, proton conduction in YSZ was reported already at room temperature in humid atmospheres, whereas oxygen conduction for YSZ was only observed for higher temperatures³². This is accompanied by

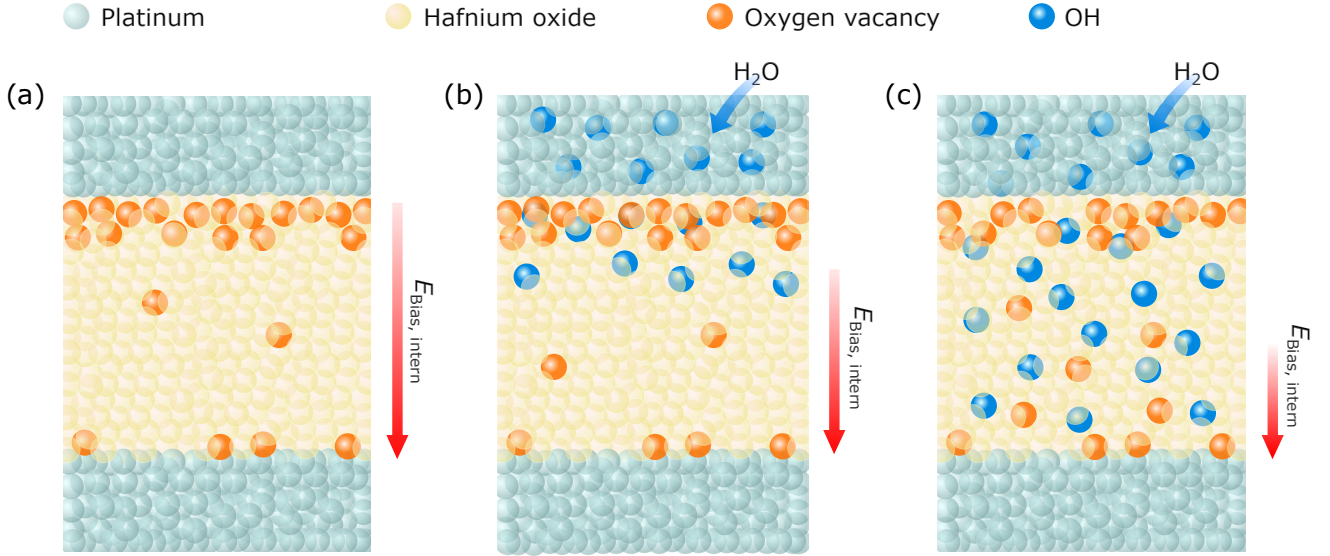


FIG. 7. a) Pristine state: Oxygen vacancies are accumulated at the top interface resulting in an internal bias field directed from the top electrode to the bottom electrode. b) Electrical cycling in wet atmosphere leads to an incorporation of protons and OH^- via equation (1). c) Further electrical cycling leads to a redistribution of protons which further reduces the bias field.

the fact that reaction (1) is exothermic for perovskite⁴⁴, but electrons must be provided by an external voltage source for the incorporation of oxygen according to reaction (2).

Together with our experimental observations that the influence of humidity or ambient air with 21 % oxygen on the remnant polarization is increased compared to 70 % dry oxygen atmosphere, we assume that either the influence and/or the incorporation of moisture is enhanced compared to oxygen incorporation. However, further measurements on the would be necessary in order to investigate the influence of oxygen in detail.

E. Kinetic Monte Carlo Simulation

To underline our model idea that we introduced before, we developed a simple one-dimensional Kinetic Monte Carlo (1D KMC) simulation model. With the help of this simulation model, we were able to investigate the influence of oxygen vacancies and protons, as well as their movement, on the electrical potential in the HfO_x thin film. The electrical potential is directly connected with the local electric field, which is responsible for the imprint mechanism in ferroelectric HfO_x films. Since our model is based on an internal bias field that is reduced in presence of protons, we have attempted to test our model theory by appropriate simulations.

The central part of our simulation model is a 25 nm thick film of HfO_x with a width of 25 μm in each direction, sandwiched between two identical electrodes. The thickness and electrode sizes are similar to the experimental conditions. The oxide film is divided into 50 identical layers of 0.5 nm length each, which corresponds to the typical lattice constant and so to the diffusion lengths of ions in HfO_x ³⁷. Each layer can consist of

a specific number of twice positively charged oxygen vacancies and singly positive charged protons. In order to obtain the electrical potential, the one-dimensional Poisson equation

$$\frac{\partial^2 \Phi(x)}{\partial x^2} = -\frac{\rho(x)}{\epsilon_0 \epsilon_r} - V_{\text{ext}}(x) \quad (4)$$

is solved, where the charge density $\rho(x)$ can be calculated by the number of defects in each layer, the permittivity ϵ_r is known from the literature⁴⁵ and $V_{\text{ext}}(x)$ is the externally applied voltage at the top electrode ($x = 0$). As we are interested in the time evolution of the defects and their effect on the electrical potential, we calculate transition rates for the defects jumping from one layer forward or reverse to a neighbouring layer via the Mott-Gurney law^{46,47}

$$R^{f/r} = N \cdot f \cdot \exp\left(-\frac{\Delta W_A^{f/r}}{k_B T}\right), \quad (5)$$

where the effective hopping barrier is modulated depending on the local potential difference between the two layers via

$$\Delta W_A^{f/r} = \Delta W_A \mp z \cdot \frac{\Delta \Phi}{2}. \quad (6)$$

Here, N denotes the number of defects (oxygen vacancies or protons) per layer, f is the attempt frequency, ΔW_A is the activation energy and z is the charge of oxygen vacancies or protons. Finally, randomly but weighted by the transition rates, one of the processes is chosen, fulfilled and the simulation time is updated via

$$t_{\text{jump}} = -\frac{\ln r_1}{\Sigma R} \quad (7)$$

TABLE I. Simulation Parameters

Symbol	Value	Symbol	Value
$\Delta W_A(\text{ox.vac.})$	0.75 eV	T	300 K
$\Delta W_A(\text{proton})$	0.60 eV	ϵ_r	30
$z(\text{ox.vac.})$	+2	f	2e13 Hz
$z(\text{proton})$	+1		

with r_1 being a random number between 0 and 1. All parameters used in the simulation are given in Table 1.

As sketched in FIG. 7 before, we expect oxygen vacancies close to the top electrode to be responsible for an internal bias field leading to a locally reduced applied electric field and a hindered ferroelectric switching. Thus, we place oxygen vacancies into the HfO_x with a linearly decreasing number from the top electrode to a distance of 5 nm. **Subsequently, simulations are performed without an applied external field to determine a possible redistribution of oxygen vacancies and protons. During the simulations, the oxygen vacancies slightly resort and even move closer to the electrodes. The same procedure was done for a starting configuration, where 25 % of the oxygen vacancies were replaced by each two protons and which showed similar results. The shape of the potential caused by the charge carrier distribution hinders protons and oxygen vacancies to redistribute uniformly within the oxide without an external field applied. The final state which has established after time is then relatively stable without external influences and is used as starting point for the following simulations.**

In FIG. 8 a), the potential of this starting configuration (identical for both cases) is shown in the dark blue curve. Resulting from the charged ions, a potential difference of approx. 2.5 V is generated from close to the top electrode to the bottom electrode. This potential difference would strongly reduce an externally applied field and so hinder the ferroelectric switching in one direction. Furthermore, we applied an AC voltage with a frequency of 1 kHz and an amplitude of 6 V to the top electrode for both cases, with and without protons. The number of cycles was set to 100, at which ferroelectric switching peaks begin to develop experimentally in humid atmosphere (see FIG. 5). Whereas in the scenario without protons no big changes occur as can be seen in the black dashed line in FIG. 8 a), the potential peak strongly decreases and the potential curve flattens during cycling for the scenario with oxygen vacancies and protons (colour gradient).

During the cycling in the scenario with oxygen vacancies and protons, the protons quickly move away from the top electrode due to their lower activation energy and distribute over the whole oxide and over time even accumulate at the bottom electrode (see FIG. 8 c)). This clearly reduces the potential peak, which additionally makes it easier for the comparatively slow oxygen vacancies to move away from the top electrode (cf. FIG. 8 b)). When only oxygen vacancies are present as mobile species, the oxygen vacancies hardly move away from the top electrode due to their higher activation energy and their initial distribution (not shown here) leads to a constantly high

potential difference. It should be mentioned that simulations using a uniform distribution of oxygen vacancies close to the top electrode instead of a linearly decreasing distribution led to similar simulation results, which are not shown here. These simulation results nicely go along with the experimental findings and the model idea introduced before. We showed that the addition of protons lead to a lowering of the potential difference over the HfO_x film and thus to a reduction of the internal field responsible for the strong observed imprint during cycling. Consequently, in the presence of an internal field, ferroelectric switching is favored in humid atmosphere.

F. Frequency dependence and fabrication impact

Further experiments are performed to investigate the frequency dependence of the wake up effect. When applying a frequency of 100 kHz in ambient atmosphere, similar to measurements in vacuum, no strong wake up effect is observable for the first 2000 cycles (see FIG. 9 a)). Unlike to measurements performed at 1 kHz, the higher frequency results in the fact that the voltage is not applied long enough to redistribute protons or oxygen vacancies. As a consequence, the internal field is not reduced and no hysteresis is formed (compare inlet Fig. 9 a)). By increasing the voltage to 8 V which is here applied to the bottom electrode (the internal field shifts the coercive voltage to higher positive values), switching peaks are recognizable after 2000 cycles and a positive coercive voltage of 6.15 V can be extracted (FIG. 9 b)). **However, a strong shift of the hysteresis (inlet Fig. 9 a)) along the x-axis is still observed, indicating that the internal bias field is still strongly present after 2000 cycles which can be attributed to the higher cycling frequency and the slower redistribution of protons.** We identify a voltage shift around 2 V compared to measurements taken at 1 kHz. The results of the frequency-dependent measurements support our assumption, that moisture clearly contributes to reducing the imprint effect. The imprint effect is a common failure mechanism of ferroelectrics that result in degraded device performance. To prevent an internal field from developing that would cause the hysteresis shift along the voltage axis, the asymmetric distribution of oxygen vacancies must be suppressed. Therefore, a thin HfO_x film is deposited with the same parameters, but annealed in 50 % oxygen/50 % nitrogen atmosphere (structural information in FIG. S4 in Supplementary Material). According to Ref. 22 the formation of oxygen vacancies is not so highly favored when the annealing is carried out in oxygen-rich atmospheres resulting in a lower bias field compared to samples annealed in nitrogen atmosphere. In FIG. 10 a), the corresponding hysteresis of the sample which is annealed in oxygen is illustrated for measurements taken in vacuum and in ambient atmosphere after 1000 cycles. In contrast to the film annealed in nitrogen, the sample shows ferroelectric switching behavior for lower applied voltages in vacuum with comparable polarization values as in humidity and the coercive voltages are similar for vacuum and ambient atmosphere. Annealing in oxygen-rich atmosphere leads to a lowering or even preventing of the internal bias field caused during deposition in the thin films.

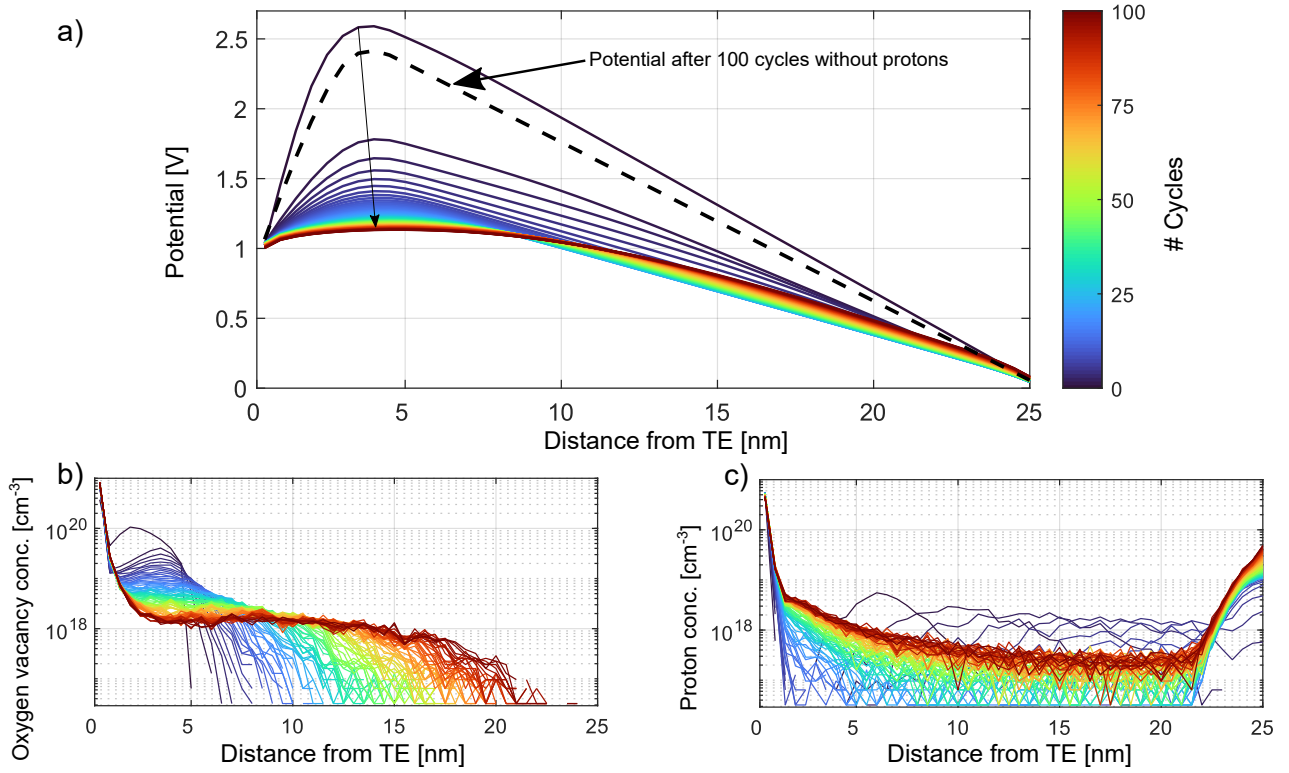


FIG. 8. a) Potential evolution in HfO_x during cycling. The high initial potential peak is strongly reduced during cycling of the cell with oxygen vacancies and protons, whereas the effect is much lower in the simulations without protons (dashed line). In b) and c), the evolution of the oxygen vacancy and the proton distributions during cycling are presented.

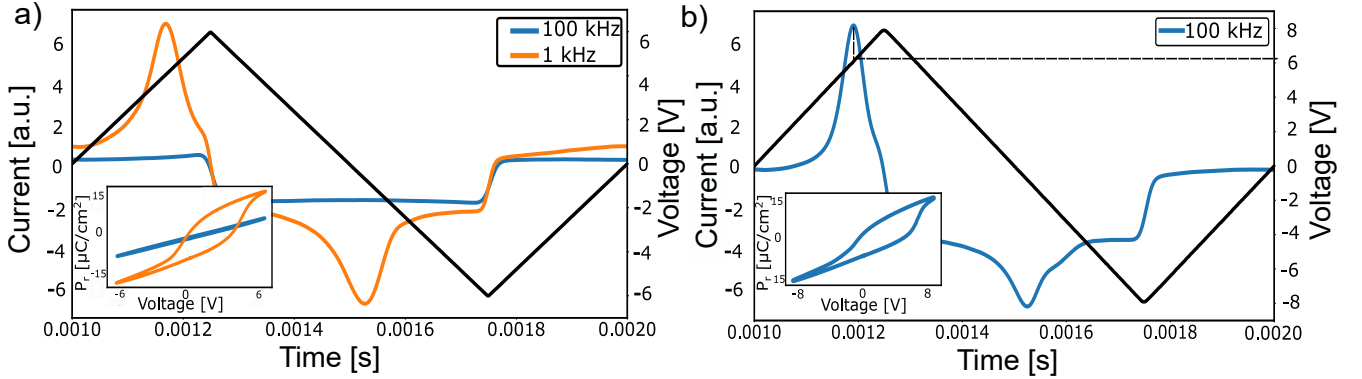


FIG. 9. a) Measurements of the switching current taken after 2000 cycles at frequencies of 1 kHz and 100 kHz and for an applied voltage of 6 V. In the inset figure, the resulting polarization in form of hysteresis are shown. b) Switching current taken at a frequency of 100 kHz and at an increased excitation voltage of 8 V.

G. Influence on conductivity

Apart from its effect on the ferroelectric behavior, moisture also affects the leakage current and the resulting conductivity. In literature²¹, it has been shown that OH^- can contribute to the ionic current and thus increase the total conductivity $\sigma_{\text{total}} = \sigma_{\text{electronic}} + \sigma_{\text{ionic}}$. In this work, leakage current measurements were performed to draw conclusions about conductivity under humidity. The applied voltage was chosen to be 1 V to prevent redox peaks

due to electrochemical processes which has been reported for hafnium oxide in Ref 40. In Fig. 11, measurements of the leakage current are shown taken in vacuum, in dry nitrogen, in a dry nitrogen/oxygen mix (30 %/70 %), under 30 % humidity, 50 % humidity and 70 % humidity conditions. In vacuum, the film exhibits the highest leakage current. The addition of dry nitrogen slightly reduces the leakage current, and a further reduction in leakage current is observed with a mixture of dry oxygen and nitrogen. Humid atmospheres lead to a stronger decrease in leakage

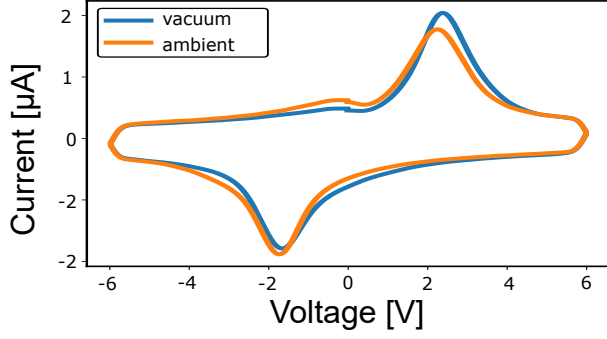


FIG. 10. Ferroelectric HfO_x thin film annealed in 50 % oxygen/ 50 % nitrogen atmosphere and measured in vacuum and in ambient atmosphere.

current compared to vacuum, which is significant at 50 % moisture. With increasing the humidity content to 70 %, the leakage current increases slightly again.

The increase in leakage current and decrease in conductivity for lower amounts of humidity has been observed before for ZnO in Ref 21. It is known from literature that for the stabilization of the ferroelectric phase in undoped HfO_x , oxygen vacancies are relevant^{17,22}. Furthermore, HfO_x is also used as a known resistive switching material, which is also based on the migration of oxygen vacancies⁴⁸. Thus, it can be assumed that the hafnium oxide prepared in our work is n-doped due to the presence of oxygen vacancies. According to Ref 21 and theoretical calculations made in Ref 49 the incorporation of OH^- leads to the appearance of deep surface states at the top of the valence band which acts as electron traps leading to band bending. This results in a barrier to the current transport along the grain size and in a reduction of the leakage current. For increasing amount of moisture though, more protons are incorporated into the thin film which leads to an increase in the ionic conduction contributing to the total conductivity and to the observed increase in leakage current for 70 % humidity.

The slight decrease in leakage current under dry nitrogen and oxygen atmosphere can be attributed, on the one hand, to the increase of relative humidity to 4 % and thus to the incorporation of OH^- . On the other hand, for the dry oxygen atmosphere, oxygen can be incorporated into the film, resulting in an annihilation of oxygen vacancies and a decrease of the leakage current. However, similar to the effect on ferroelectric properties, the effect is not as pronounced as in humid atmospheres.

IV. CONCLUSION

We presented for the first time a detailed study on the influence of different atmospheres on the ferroelectric switching behavior of undoped HfO_x thin films. At the same field strength, the wake up effect and thus ferroelectric switching is suppressed in vacuum and dry atmosphere, while the film

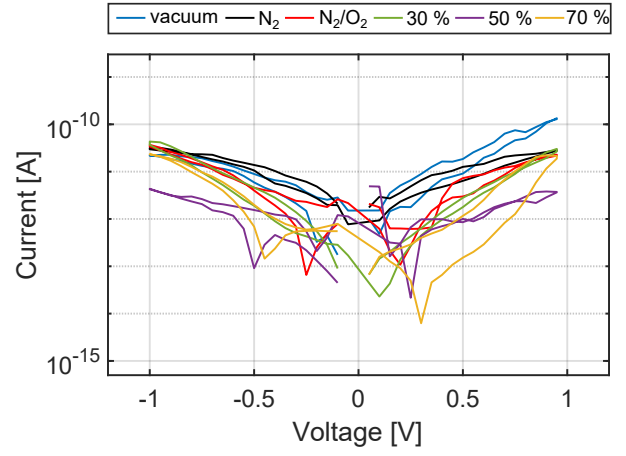


FIG. 11. Leakage current measurements. For vacuum the highest leakage current is measured. With increasing moisture content, the leakage current is reduced due to charge trapping.

shows a remanent polarization between 14 and 25 $\mu\text{C}/\text{cm}^2$ in humid atmospheres. However, ferroelectric switching in vacuum can be achieved by increasing the excitation voltage. We attribute this effect to an initial distribution of oxygen vacancies causing an internal bias field and imprint in the thin film due to nitrogen annealing. In humid atmospheres, protons can be incorporated in the thin film and lead to a decrease of the bias field due to their redistribution under the application of an electric field which reduces the imprint. KMC simulations showed that the proton movement leads to a lowering of the potential and thus of the internal field which allows the oxygen vacancies to redistribute within the oxide layer. The level of humidity influences the duration of the wake up effect since more incorporated protons result in a faster redistribution. Annealing in oxygen atmosphere can prevent the creation of oxygen vacancies accumulation at the interface and thus the resulting imprint effect. **Additional measurements of the leakage current in different levels of humidity showed that moisture also affects the resulting conductivity.**

SUPPLEMENTARY MATERIAL

See the supplementary material for figures S1-S5. Additional information on the direction of the internal bias field and the effect of additional heating during evacuation as well as structural information can be found in the supplementary material.

ACKNOWLEDGMENTS

This work was funded by the German Research Foundation (Deutsche Forschungsgemeinschaft) within the scope of the project "Zeppelin" (Project No. BO 1629/12).

DATA AVAILABILITY STATEMENT

The data that support the findings of this study are available within the article and its Supplementary Material.

COMPETING INTERESTS

The authors have no conflict of interest to declare.

REFERENCES

- ¹T. Böske, J. Müller, D. Bräuhäus, U. Schröder, and U. Böttger, "Ferroelectricity in hafnium oxide thin films," *Applied Physics Letters* **99** (2011).
- ²T. Böske, J. Müller, D. Bräuhäus, U. Schröder, and U. Böttger, "Ferroelectricity in hafnium oxide: Cmos compatible ferroelectric field effect transistors," in *2011 International electron devices meeting (IEEE, 2011)* pp. 24–5.
- ³U. Schroeder, S. Mueller, J. Mueller, E. Yurchuk, D. Martin, C. Adelmann, T. Schloesser, R. van Bentum, and T. Mikolajick, "Hafnium oxide based cmos compatible ferroelectric materials," *ECS Journal of Solid State Science and Technology* **2**, N69 (2013).
- ⁴X. Sang, E. D. Grimley, T. Schenk, U. Schroeder, and J. M. LeBeau, "On the structural origins of ferroelectricity in HfO₂ thin films," *Applied Physics Letters* **106** (2015).
- ⁵R. Materlik, C. Künneth, and A. Kersch, "The origin of ferroelectricity in Hf_{1-x}Zr_xO: A computational investigation and a surface energy model," *Journal of Applied Physics* **117** (2015).
- ⁶Y. Wei, P. Nukala, M. Salverda, S. Matzen, H. J. Zhao, J. Momand, A. S. Everhardt, G. Agnus, G. R. Blake, P. Lecoeur, *et al.*, "A rhombohedral ferroelectric phase in epitaxially strained Hf_{0.5}Zr_{0.5}O₂ thin films," *Nature materials* **17**, 1095–1100 (2018).
- ⁷P. Nukala, Y. Wei, V. de Haas, Q. Guo, J. Antoja-Lleonart, and B. Noheda, "Guidelines for the stabilization of a polar rhombohedral phase in epitaxial Hf_{0.5}Zr_{0.5}O₂ thin films," *Ferroelectrics* **569**, 148–163 (2020).
- ⁸D. Zhou, J. Xu, Q. Li, Y. Guan, F. Cao, X. Dong, J. Müller, T. Schenk, and U. Schröder, "Wake-up effects in si-doped hafnium oxide ferroelectric thin films," *Applied Physics Letters* **103** (2013).
- ⁹T. Schenk, U. Schroeder, M. Pesic, M. Popovici, Y. V. Pershin, and T. Mikolajick, "Electric field cycling behavior of ferroelectric hafnium oxide," *ACS applied materials & interfaces* **6**, 19744–19751 (2014).
- ¹⁰M. Pešić, F. P. G. Fengler, L. Larcher, A. Padovani, T. Schenk, E. D. Grimley, X. Sang, J. M. LeBeau, S. Slesazeck, U. Schroeder, *et al.*, "Physical mechanisms behind the field-cycling behavior of HfO₂-based ferroelectric capacitors," *Advanced Functional Materials* **26**, 4601–4612 (2016).
- ¹¹M. H. Park, H. J. Kim, Y. J. Kim, Y. H. Lee, T. Moon, K. D. Kim, S. D. Hyun, and C. S. Hwang, "Study on the size effect in Hf_{0.5}Zr_{0.5}O₂ films thinner than 8 nm before and after wake-up field cycling," *Applied Physics Letters* **107** (2015).
- ¹²T. Schenk, M. Hoffmann, J. Ocker, M. Pesic, T. Mikolajick, and U. Schroeder, "Complex internal bias fields in ferroelectric hafnium oxide," *ACS applied materials & interfaces* **7**, 20224–20233 (2015).
- ¹³S. Starschich, S. Menzel, and U. Böttger, "Evidence for oxygen vacancies movement during wake-up in ferroelectric hafnium oxide," *Applied Physics Letters* **108** (2016).
- ¹⁴P. Buragohain, C. Richter, T. Schenk, H. Lu, T. Mikolajick, U. Schroeder, and A. Gruverman, "Nanoscope studies of domain structure dynamics in ferroelectric la: Hfo2 capacitors," *Applied Physics Letters* **112** (2018).
- ¹⁵F. P. Fengler, M. Pešić, S. Starschich, T. Schneller, U. Böttger, T. Schenk, M. H. Park, T. Mikolajick, and U. Schroeder, "Comparison of hafnia and pzt based ferroelectrics for future non-volatile fram applications," in *2016 46th European Solid-State Device Research Conference (ESSDERC) (IEEE, 2016)* pp. 369–372.
- ¹⁶F. Huang, X. Chen, X. Liang, J. Qin, Y. Zhang, T. Huang, Z. Wang, B. Peng, P. Zhou, H. Lu, *et al.*, "Fatigue mechanism of yttrium-doped hafnium oxide ferroelectric thin films fabricated by pulsed laser deposition," *Physical Chemistry Chemical Physics* **19**, 3486–3497 (2017).
- ¹⁷T. Mittmann, M. Michailow, P. D. Lomenzo, J. Gärtner, M. Falkowski, A. Kersch, T. Mikolajick, and U. Schroeder, "Stabilizing the ferroelectric phase in HfO₂-based films sputtered from ceramic targets under ambient oxygen," *Nanoscale* **13**, 912–921 (2021).
- ¹⁸M. Materano, P. D. Lomenzo, A. Kersch, M. H. Park, T. Mikolajick, and U. Schroeder, "Interplay between oxygen defects and dopants: effect on structure and performance of HfO₂-based ferroelectrics," *Inorganic Chemistry Frontiers* **8**, 2650–2672 (2021).
- ¹⁹U. Schroeder, M. Materano, T. Mittmann, P. D. Lomenzo, T. Mikolajick, and A. Toriumi, "Recent progress for obtaining the ferroelectric phase in hafnium oxide based films: impact of oxygen and zirconium," *Japanese Journal of Applied Physics* **58**, SL0801 (2019).
- ²⁰M. Lederer, P. Bagul, D. Lehniger, K. Mertens, A. Reck, R. Olivo, T. Kampfe, K. Seidel, and L. M. Eng, "Influence of annealing temperature on the structural and electrical properties of si-doped ferroelectric hafnium oxide," *ACS Applied Electronic Materials* **3**, 4115–4120 (2021).
- ²¹G. Milano, M. Luebben, M. Laurenti, S. Porro, K. Bejtka, S. Bianco, U. Breuer, L. Boarino, I. Valov, and C. Ricciardi, "Ionic modulation of electrical conductivity of zno due to ambient moisture," *Advanced Materials Interfaces* **6**, 1900803 (2019).
- ²²F. Berg, J. Lübben, and U. Böttger, "Parameters for ferroelectric phase stabilization of sputtered undoped hafnium oxide thin films," *Japanese Journal of Applied Physics* **62**, 015507 (2023).
- ²³Q. Ma, H. He, and Y. Liu, "In situ drifts study of hygroscopic behavior of mineral aerosol," *Journal of Environmental Sciences* **22**, 555–560 (2010).
- ²⁴P. Kubelka and F. Munk, "An article on optics of paint layers," *Z. Tech. Phys* **12**, 259–274 (1931).
- ²⁵M. Lucarini, A. Durazzo, J. Kiefer, A. Santini, G. Lombardi-Boccia, E. B. Souto, A. Romani, A. Lampe, S. Ferrari Nicoli, P. Gabrielli, *et al.*, "Grape seeds: chromatographic profile of fatty acids and phenolic compounds and qualitative analysis by ftir-atr spectroscopy," *Foods* **9**, 10 (2019).
- ²⁶S. Chemchoub, L. Oularbi, A. El Attar, S. A. Younsi, F. Bentiss, C. Jama, and M. El Rhazi, "Cost-effective non-noble metal supported on conducting polymer composite such as nickel nanoparticles/polypyrrole as efficient anode electrocatalyst for ethanol oxidation," *Materials Chemistry and Physics* **250**, 123009 (2020).
- ²⁷T. Szyjka, L. Baumgarten, T. Mittmann, Y. Matveyev, C. Schlueter, T. Mikolajick, U. Schroeder, and M. Muller, "Enhanced ferroelectric polarization in tin/HfO₂/tin capacitors by interface design," *ACS Applied Electronic Materials* **2**, 3152–3159 (2020).
- ²⁸W. Hamouda, F. Mehmood, T. Mikolajick, U. Schroeder, T. O. Mendes, A. Locatelli, and N. Barrett, "Oxygen vacancy concentration as a function of cycling and polarization state in tin/Hf_{0.5}Zr_{0.5}O₂/tin ferroelectric capacitors studied by x-ray photoemission electron microscopy," *Applied Physics Letters* **120** (2022).
- ²⁹M. Copel, R. P. Pezzi, D. Neumayer, and P. Jamison, "Reduction of hafnium oxide and hafnium silicate by rhenium and platinum," *Applied physics letters* **88** (2006).
- ³⁰G. Milano, M. Luebben, M. Laurenti, L. Boarino, C. Ricciardi, and I. Valov, "Structure-dependent influence of moisture on resistive switching behavior of zno thin films," *Advanced Materials Interfaces* **8**, 2100915 (2021).
- ³¹I. Valov and T. Tsuruoka, "Effects of moisture and redox reactions in vcm and ecm resistive switching memories," *Journal of Physics D: Applied Physics* **51**, 413001 (2018).
- ³²S. Kim, H. J. Avila-Paredes, S. Wang, C.-T. Chen, R. A. De Souza, M. Martin, and Z. A. Munir, "On the conduction pathway for protons in nanocrystalline yttria-stabilized zirconia," *Physical Chemistry Chemical Physics* **11**, 3035–3038 (2009).
- ³³A. Marinopoulos, "Protons in cubic yttria-stabilized zirconia: Binding sites and migration pathways," *Solid State Ionics* **315**, 116–125 (2018).
- ³⁴S. Menzel, M. Von Witzleben, V. Havel, and U. Böttger, "The ultimate switching speed limit of redox-based resistive switching devices," *Faraday discussions* **213**, 197–213 (2019).
- ³⁵S. Zafar, H. Jagannathan, L. F. Edge, and D. Gupta, "Measurement of oxygen diffusion in nanometer scale hfo2 gate dielectric films," *Applied Physics Letters* **98** (2011).

- ³⁶R. He, H. Wu, S. Liu, H. Liu, X. R. Wang, and Z. Zhong, "Charged oxygen vacancy induced ferroelectric structure transition in hafnium oxide," arXiv preprint arXiv:2106.12159 (2021).
- ³⁷N. Kopperberg, S. Wiefels, S. Liberda, R. Waser, and S. Menzel, "A consistent model for short-term instability and long-term retention in filamentary oxide-based memristive devices," *ACS Applied Materials & Interfaces* **13**, 58066–58075 (2021).
- ³⁸J. Hinterberg, A. Adams, B. Blümich, P. Heitjans, S. Kim, Z. A. Munir, and M. Martin, "1 h-nmr measurements of proton mobility in nano-crystalline ysz," *Physical Chemistry Chemical Physics* **15**, 19825–19830 (2013).
- ³⁹M. Takayanagi, S. Furuichi, W. Namiki, T. Tsuchiya, M. Minohara, M. Kobayashi, K. Horiba, H. Kumigashira, and T. Higuchi, "Proton conduction on ysz electrolyte thin films prepared by rf magnetron sputtering," *ECS Transactions* **75**, 115 (2017).
- ⁴⁰M. Lübben, S. Wiefels, R. Waser, and I. Valov, "Processes and effects of oxygen and moisture in resistively switching taox and hfox," *Advanced electronic materials* **4**, 1700458 (2018).
- ⁴¹J. Schaeffer, L. Fonseca, S. Samavedam, Y. Liang, P. Tobin, and B. White, "Contributions to the effective work function of platinum on hafnium dioxide," *Applied physics letters* **85**, 1826–1828 (2004).
- ⁴²R. P. Pezzi, M. Copel, M. Gordon, E. Cartier, and I. J. R. Baumvol, "Oxygen transport and reaction mechanisms in rhenium gate contacts on hafnium oxide films on si," *Applied physics letters* **88** (2006).
- ⁴³J.-J. Ganem, I. Trimaille, I. Vickridge, D. Blin, and F. Martin, "Study of thin hafnium oxides deposited by atomic layer deposition," *Nuclear Instruments and Methods in Physics Research Section B: Beam Interactions with Materials and Atoms* **219**, 856–861 (2004).
- ⁴⁴K.-D. Kreuer, "Proton-conducting oxides," *Annual Review of Materials Research* **33**, 333–359 (2003).
- ⁴⁵E. D. Grimley, T. Schenk, X. Sang, M. Pešić, U. Schroeder, T. Mikolajick, and J. M. LeBeau, "Structural changes underlying field-cycling phenomena in ferroelectric HfO₂ thin films," *Advanced Electronic Materials* **2**, 1600173 (2016).
- ⁴⁶N. Kopperberg, S. Wiefels, K. Hofmann, J. Otterstedt, D. J. Wouters, R. Waser, and S. Menzel, "Endurance of 2 mbit based beol integrated reram," *IEEE Access* **10**, 122696–122705 (2022).
- ⁴⁷C. La Torre, A. F. Zurhelle, T. Breuer, R. Waser, and S. Menzel, "Compact modeling of complementary switching in oxide-based reram devices," *IEEE transactions on electron devices* **66**, 1268–1275 (2019).
- ⁴⁸W. Banerjee, A. Kashir, and S. Kamba, "Hafnium oxide (hfo2)—a multifunctional oxide: a review on the prospect and challenges of hafnium oxide in resistive switching and ferroelectric memories," *Small* **18**, 2107575 (2022).
- ⁴⁹S. Porro, F. Risplendi, G. Cicero, K. Bejtka, G. Milano, P. Rivolo, A. Jamin, A. Chiolerio, C. F. Pirri, and C. Ricciardi, "Multiple resistive switching in core-shell zno nanowires exhibiting tunable surface states," *Journal of Materials Chemistry C* **5**, 10517–10523 (2017).
- ⁵⁰R. Merkle and J. Maier, "How is oxygen incorporated into oxides? a comprehensive kinetic study of a simple solid-state reaction with struo3 as a model material," *Angewandte Chemie International Edition* **47**, 3874–3894 (2008).